Published by :
https://www.ijert.org/
An International Peer-Reviewed Journal

International Journal of Engineering Research & Technology (IJERT)
ISSN: 2278-0181
Vol. 15 Issue 05 , May - 2026

Study of medium-range ordering in Zr-Cu and Zr-Cu-M (M = Al, Ag) alloys

Jayraj P. Anadani[1]
[1] Department of Physics, Sardar Patel University, Vallabh Vidyanagar, India

Abstract - In metallic glasses, medium-range order (MRO) is responsible for governing the glass-forming ability, structural stability, and dynamical arrest. However, the systematic characterization of MRO continues to be challenging due to the complexity of polyhedral interconnectivity beyond the first coordination shell. In this study, we use the LAMMPS software for classical molecular dynamics simulations to study the MRO in binary Cu-Zr and ternary Zr-Cu-M (M = Al, Ag) metallic glasses. Full icosahedra (FI), ⟨0,0,12,0⟩, are identified as the dom-inant short-range structural motifs using Voronoi tessellation, and their connectivity by vertex-sharing (VS), edge-sharing (ES), face-sharing (FS), and bi-cap sharing (BS) mechanisms is systematically examined various compositions. BS and FS are found to be the most popular FI connectivity methods for binary Cu_xZr_{100-x}, $46 \leq x \leq 70$ glasses, while ES is still the least preferred. As the Cu content increases, the FI population grows rapidly, resulting in microscopic percolating icosahedral networks. Ag promotes compact weakly linked clusters and crystal-like MRO in ternary systems, whereas Al encourages icosahedral MRO through hetero-coordination. It has been confirmed by statis-tical heat maps of polyhedral connectivity that Cu-rich alloys exhibit higher icosahedral diversity, while Zr-rich systems exhibit crystal-like ordering. These findings provide a coherent framework that connects topological organization, chemical ordering, and composition at the MRO scale in metallic glass-forming systems.

Keywords -Metallic glasses, molecular dynamics, Cu-Zr, glass-forming ability, medium-range order, icosahedral connectivity, Voronoi Analysis

1. INTRODUCTION

In metallic glasses, the medium-range order (MRO) occupies the structural hierarchy between nearest-neighbor coordination and the absence of true long-range periodicity, while capturing the complex interactions and arrangements of these local structural motifs (polyhedra) as they interconnect, cluster, and structure one another over longer distances that extend beyond the initial coordination shell [1–9]. While short-range order identifies the topology of individual coordination polyhedra, MRO concerns the spatial correlation, interconnectivity, and orientational coherence among these polyhedra over length scales extending beyond a single atomic shell. This level of organization is now widely regarded as crucial for understanding vitrification, k inetic a rrest, s tructural heterogeneity, and the emergence of mechanically and thermodynamically stable amorphous states [10–13]. In particular, metallic glasses containing strong fivefold local symmetry often develop networks of interconnected icosahedral or quasi-icosahedral units, and such networks are known to frustrate crystallization by creating topologies incompatible with translationally periodic crystalline order [14, 15]. This distinction holds a major role as numerous vital characteristics of metallic glasses, such as glass-forming ability (GFA), thermal stability, elastic response, and deformation behavior, are associated not only with the existence of preferred local motifs like icosahedral-like clusters, but also with the spatial correlation and connectivity of these motif types [10, 16–21]. As a result, a comprehensive structural analysis should go beyond just the identification of isolated local polyhedra, looking into the topology, extent, and connectivity of networks based on motifs [22].

A substantial body of literature has therefore moved beyond the identification of dominant Voronoi polyhedra toward the study of their collective organization. Efficient cluster packing models based on the packing of the solute-centered local structural motifs have been proposed to describe the structure of the metallic glasses at the MRO scale [1, 2]. While the generality of these models have been debated, various aspects of the interconnection among the dominant polyhedra types at the MRO scale have been investigated from the viewpoint of glass formation and structure-property relationship in metallic glasses [16]. In Cu–Zr-based metallic glasses, icosahedral clusters have been reported not merely as isolated short-range motifs, but as constituents of extended medium-range networks formed through vertex-, edge-, face-, and volume-sharing connections [4,23–35]. Although a significant number of studies report the investigation of the atomic-level structure of the binary Cu-Zr and ternary Zr-Cu-M (M being a transition metal element) metallic glasses at SRO and MRO scale, systematic studies of the compositional variations and the chemical effects of minor alloying of a third transition metal element on the interconnectivity of the dominant local structural motifs in the binary Cu-Zr alloys are still scarce.

It is well known that the glass formation and structural stability of Zr–Cu-based metallic glasses are governed by a subtle interplay between atomic packing, chemical short-range order, and electronic effects. In the binary Cu–Zr system, the analysis of local coordination environments showed that icosahedral and icosahedra-like clusters, particularly the full icosahedron $< 0, 0, 12, 0 >$ and related Frank–Kasper polyhedra such as $< 0, 2, 8, 2 >$, are the dominant short-range structural motifs.

International Journal of Engineering Research & Technology (IJERT)
ISSN: 2278-0181
Vol. 15 Issue 05 , May - 2026

Their populations, distortion, packing efficiency, and stoichiometric preference were shown to vary sensitively with composition, and these variations were linked to the glass-forming ability of the alloy. In addition, the investigations of ternary Zr–Cu–M (M=Al/Ag) systems emphasized that microalloying elements such as Al and Ag modify chemical short-range order in qualitatively different ways, thereby influencing not only local topology but also the electronic stabilization of the amorphous state. Together, these results make it clear that a description based solely on isolated local clusters is incomplete; what is equally important is how these clusters interconnect beyond the first coordination shell to generate MRO. In this study, we present the study of the MRO in the two metallic glass systems where the primary focus is on investigating the interconnectivity among the icosahedral polyhedra $< 0, 0, 12, 0 >$. We look into the distributions of the four icosahedron connectivity mechanisms (explained in Sec. 2.2), number and sizes of icosahedral clusters that are formed through these interconnection mechanisms.

2. METHODS

2.1 Classical Molecular Dynamics Simulations

Classical molecular dynamics (MD) simulations were carried out using the LAMMPS package [36]. The simulation workflow i s e volved i n t hree d istinct p hases: (i) a n i nitial high-temperature equilibration in the liquid state, (ii) a rapid cooling of the liquid to the glassy state, and (iii) production runs to record atomic trajectories at 300 K for structural analysis. The initial configurations w ere g enerated b y randomly placing atoms in cubic simulation cells with periodic boundary conditions applied in all three dimensional axes. Binary Cu_xZr_{100-x}, (x = 46, 50, 54, 58, 62, 64, 66, and 70) metallic alloys are investigated with each composition comprising total 4000 atoms. In the case of ternary Zr-Cu-M (M=Al, Ag) systems, four compositions, $Zr_{50}Cu_{40}Al_{10}$, $Cu_{50}Zr_{40}Al_{10}$, $Zr_{50}Cu_{40}Ag_{10}$, and $Cu_{50}Zr_{40}Ag_{10}$, have been studied with each composition having 13,500 atoms. To begin with, each of these systems were equilibrated at a temperature of 2000 K for a duration of 1 ns within the isothermal-isobaric (NPT) ensemble, employing a Nose-Hoover thermostat and barostat [37,38]. The external pressure was maintained at zero throughout the simulations. Following the equilibration phase, the systems were subjected to a rapid cooling from 2000 K to 300 K at the rate of 10^{12} K/s. The equations of motion were precisely integrated through the velocity-Verlet algorithm, employing a time step of 1-2 fs [39]. In order to enhance statistical reliability, an additional production run was carried out in the NPT ensemble following the quench to 300 K. The quenched structures were subsequently relaxed through energy minimization via the conjugate-gradient algorithm [40], hoping to guide the system toward a local minimum on the potential energy landscape [41]. The structural analyses presented in this study were conducted on the optimized inherent structures instead of the fluctuating thermal c onfigurations. This method effectively reduces thermal noise, enabling a more accurate characterization of the fundamental short-range and medium-range structural motifs [42].

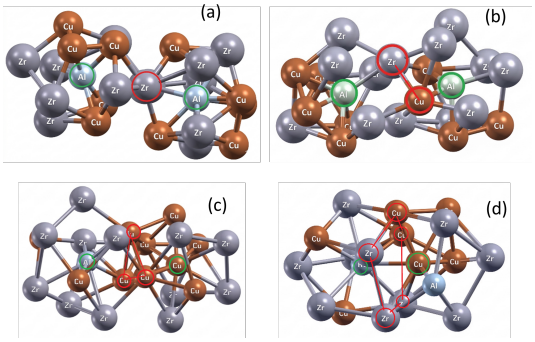

Figure 1: Four basic mechanisms for connectivity between the full icosahedra $< 0, 0, 12, 0 >$, (a) vertex-sharing with one common atom, (b) edge-sharing with two common atoms, (c) face-sharing with three common atoms, and (d) bi-cap sharing with five common atoms.

2.2 Voronoi Analysis

The average structure of the amorphous metallic glasses, characterized in terms of the pair distribution function, g(r), and static structure factor, S(q), does not uniquely resolve medium-range topological organization. To examine the MRO based on the networks of the locally favoured SRO structures, the atomic-level 3D structure has been characterized using the Voronoi tessellation method [43]. A regular icosahedron is denoted by the Voronoi index $\langle 0, 0, 12, 0 \rangle$, which corresponds to a polyhedron featuring 12 pentagonal faces [2, 44, 45]. Most of the icosahedra in the metallic glasses are geometrically imperfect i.e. distorted. However, owing to all 12 faces of the Voronoi polyedra to be pentagonal, the icosahedra are often referred to as "full icosahedra (FI)". $\langle 0, 0, 12, 0 \rangle$ is one of the many polyhedra that exist in a metallic glass [4, 13]. However, as emphasised in the previous discussions, FIs are the key SRO structures linked to the MRO and dynamics of the metallic glass-forming liquids. Therefore, FI interconnectivity and networks are often investigated to understand the MRO-level clustering of these polyhedra. The FI interconnected network is formed through the four basic mechanisms: vertex-sharing (VS), edge-sharing (ES), face-sharing (FS), and pentagonal bicap-sharing (BS), [2, 45, 46] as shown in Fig. 1.

3. RESULTS AND DISCUSSION

3.1 Cu-Zr metallic glasses

3.1.1 Pair Distribution Function and Icosahedra Connectivity

The correlation between the positions of the first peak and the sub-peaks in the second peak of total g(r) signify the presence of icosahedral SRO and MRO in a metallic glass. FIs are the key SRO structures in the Cu-Zr metallic glasses. Therefore,

International Journal of Engineering Research & Technology (IJERT)
ISSN: 2278-0181
Vol. 15 Issue 05 , May - 2026

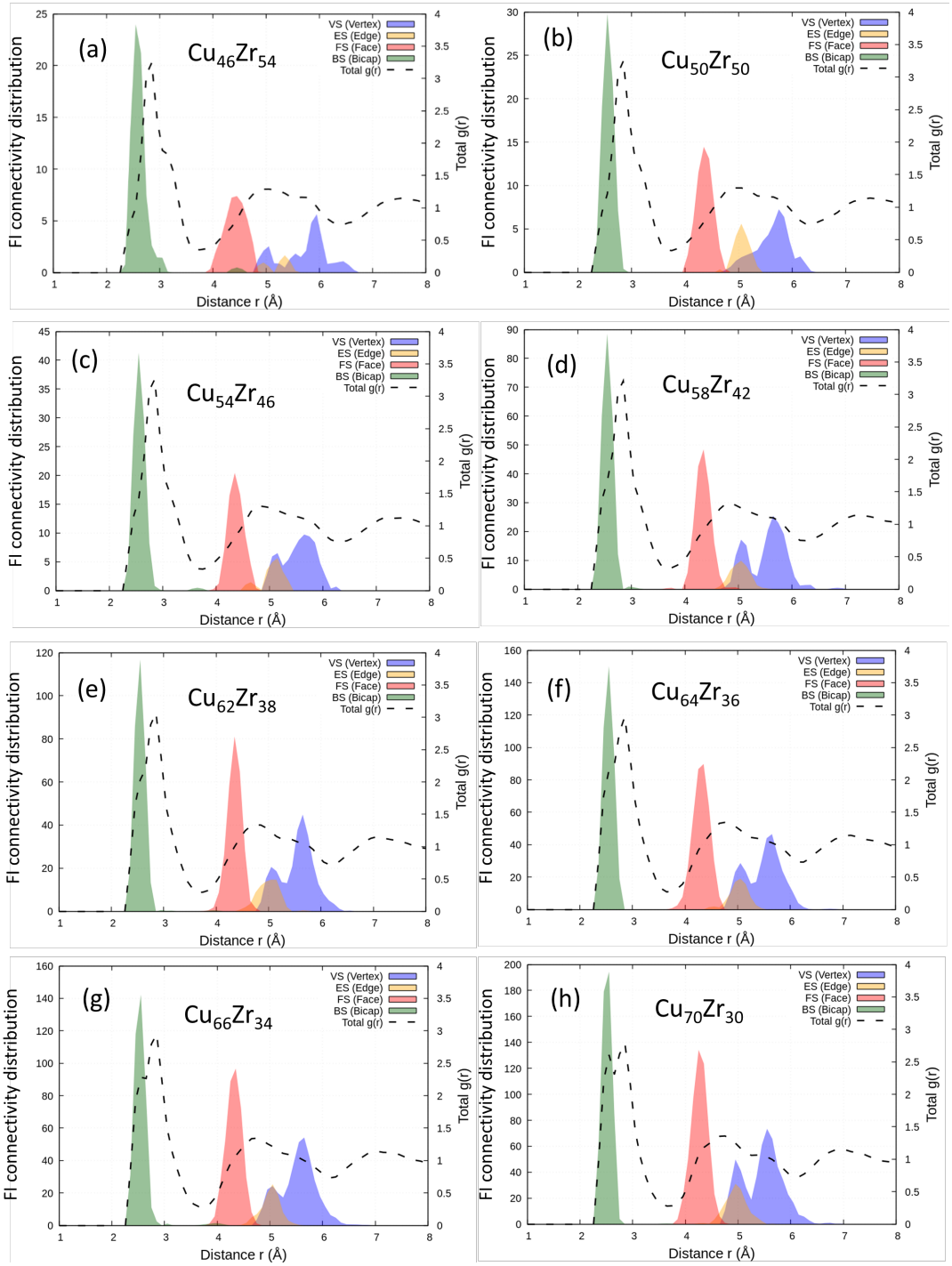

Figure 2: Total g(r) of binary metallic glasses, (a) $Cu_{46}Zr_{54}$, (b) $Cu_{50}Zr_{50}$, (c) $Cu_{54}Zr_{46}$, (d) $Cu_{58}Zr_{42}$, (e) $Cu_{62}Zr_{38}$, (f) $Cu_{64}Zr_{36}$, (g) $Cu_{66}Zr_{34}$, and (h) $Cu_{70}Zr_{30}$. The shaded curves in the figure show the distributions of the atomic pair distances of the central atoms of the FIs connected through vertex-sharing (blue), edge-sharing(orange), face-sharing (red), and bi-cap sharing (green).

the distribution of the atomic pair distances between the central atoms of two interconnected FIs through the four mechanisms provides useful insight of the degree of icosahedral SRO and MRO contributions to the average structure of the metallic glasses [25, 34, 46]. Fig. 2 show the total g(r) of eight metallic glass compositions, Cu_xZr_{100-x}, $46 \leq x \leq 70$. The distributions of pair distances between the central atoms of the FIs connected through the vertex-sharing, edge-sharing, face-sharing and bi-cap sharing mechanisms are also shown in the figure. While some general features of the FI connectivity distributions can be easily understood considering the FI connectivity mechanisms illustrated in Fig. 1, the results also provide

International Journal of Engineering Research & Technology (IJERT)
ISSN: 2278-0181
Vol. 15 Issue 05 , May - 2026

an insight of the chemical-ordering.

First, the average central atom pair distances are shortest for the BS connectivity, and essentially correspond to the Cu-Cu pair distance ($\sim$ 2.6 Å) as almost all the FIs are Cu-centred as shown in the next section. The BS connectivity increases with increasing FI population due to increase in the Cu% in the binary metallic glasses. An increase in the Cu-Cu bonding is also evident from the appearance of a left shoulder peak in the first peak of g(r).

Second, the average FI central atom pair distances in VS FI connections are the largest due to indirect central atom connectivity through a common vertex atom. The common vertex atom between two Cu-centered FIs could be a Cu or a Zr atom, and the VS connections would correspond to Cu-Cu-Cu and Cu-Zr-Cu triplets. Therefore, VS FI connections exhibit a broad bimodal distribution with a peak near $\sim$ 5.2 Åfor Cu-Cu-Cu triplets and another peak at $\sim$ 5.8 Åfor Cu-Zr-Cu triplets. As the Cu% and FI population increase in the binary glass, Cu-Cu-Cu VS connectivity becomes distinctly prominent. At the same time, it is also noteworthy that Cu-Zr-Cu connectivity remains dominant despite a significant reduction in the Zr concentration. It implies formation of a larger compact interpenetrating FI clusters through other three connectivity mechanisms apart from VS. It is clearly evident that VS connectivity among FIs significantly account for the sub-peaks of the second neighbour peak in g(r), where the second sub-peak can be mainly attributed to radial distribution of the Zr atoms at $r \sim 5.8$ Å.

Third, the triangular face-sharing(FS) with three common atoms between two FIs is the second most preferred connectivity mechanism, which is understandable when we note the standard dense atomic packing on triangular lattice in FCC and HCP crystals. The formation of icosahedra is a result of the frustration in crystallisation due to competing nucleation and growth processes of different elements of the alloys [44, 47, 48]. The average pair distance of the central FI atoms in FS in the binary glasses is found to be $\sim$ 4.3 Å. This distance is $\sim$ 1.63 times the Cu-Cu distance of $\sim$ 2.6 Å(the position of the left shoulder peak in the first peak of total g(r)) for hard-sphere-like nearest neighbour coordination. For a dense random packing of hard-spheres, the trigonal bipyramid configurations of the hard-spheres equivalent to FS mechanism are predicted to a sub-peak in the second peak of g(r) at $r = 1.63R_1$, where R_1 is the position of the first peak [49]. It has been shown that the structure of Cu-Zr systems can be modeled by an ideal hard-sphere mixture approximation [50]. The presence of the sub-peak at $r = 1.63R_1$ is usually smeared out in the average global structure of the metallic glasses due to temperature related fluctuations of the pair distances. However, the existence of this sub-peak in has been reported in pair distribution function of the inherent structures of $Cu_{64}Zr_{36}$ metallic glass where the temperature effects are quenched out [34]. Thus, the analysis of the FI connectivity bring forth the significance of FS sharing in MRO, which remains subdued due to the absence of a characteristic feature in g(r).

The fourth type of FI connectivity, the Edge-sharing, is the least favoured FI sharing mechanism in MRO due to incompatibility efficient filling of the space leading to dense atomic packing. To provide a more quantitative and comparative outlook of the four FI sharing mechanisms in the structure at the MRO scale, a plot of the percentage of FI sharing Vs. Cu% is shown in Fig. 3. It can be seen that the four FI connectivity types exhibit non-monotonic composition dependence. While the BS, FS and VS remain the most dominant connectivity mechanisms against the least favoured ES connectivity, the variation in their percentage in the vicinity of the Cu% of 50 and 64 are noteworthy from the viewpoint of the reports of best glass-forming compositions $Cu_{50}Zr_{50}$ and $Cu_{64}Zr_{36}$ correlated with the mass density [51] and atomic packing efficiency [52, 53]. It suggests that the higher BS and FS connectivities relative to the VS, ES connectivities among the FIs at the MRO scale could be linked to higher atomic packing efficiency and mass density.

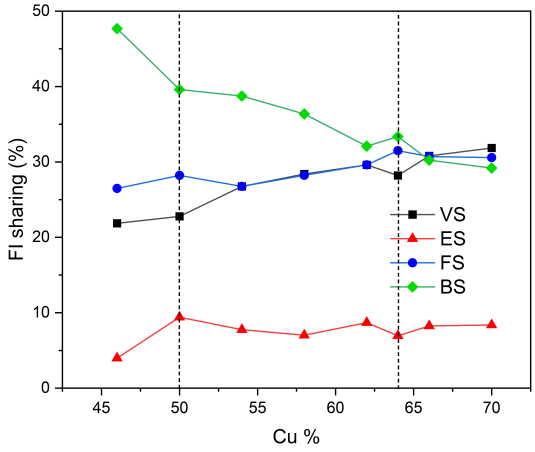

Figure 3: Percentage of FI connectivities through VS, ES, FS, and BS in Cu-Zr glasses

The last general observation from the results in Fig. 2 is the consistence prevalence of the positions of the peaks of the distributions of the four connectivity mechanisms in all the Cu-Zr glass compositions. The peak positions remain almost unchanged while the FI connectivities change with the change in FI population. It indicates the formation of a backbone structure of interpenetrating FIs at the MRO scale. FI clusters with as many as 15–20 FIs interconnected to a FI have been found to exist in a $Cu_{64}Zr_{36}$ metallic glass. The MRO backbone structure of interconnected network of FIs of the order of $\sim$ 2–3 nm have been reported to evolve in the supercooled region in $Cu_{64.5}Zr_{35.5}$ [29].

3.1.2 Full icosahedra connectivity analysis

To elucidate the icosahedral MRO in the studied metallic glasses, we have carried out a detailed analysis of the FI population, the number and size of the icosahedral clustered formed through interconnection among the FIs. It can be seen from Fig. 4(a) that FI population show a sensitive composition dependence, especially beyond Cu %>54 where FI% in the glass increases rapidly. As the FI population increases, the intercon-

International Journal of Engineering Research & Technology (IJERT)
ISSN: 2278-0181
Vol. 15 Issue 05 , May - 2026

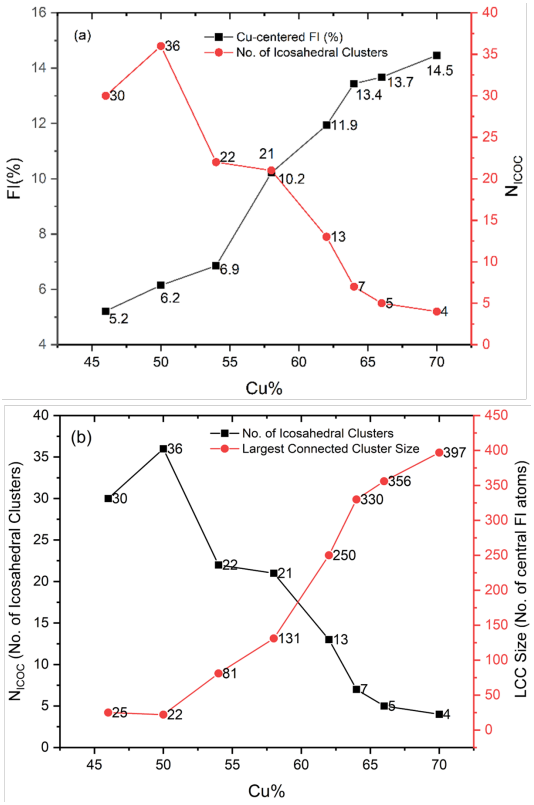

Figure 4: Full icosahedra connectivity and MRO statistics in Cu-Zr glasses, (a) FI population and number of distinct FI clusters formed by FI sharing, and (b) Number of FI clusters and the LCCs. As number of Zr-centred FIs are negligible, the percentage of FIs have been calculated with respect to the number of Cu atoms in the glass

nectivity among the FIs gives rise to larger icosahedral clusters at the MRO scale as indicated by the increasing largest connected cluster (LCC) size in Fig. 4(b), and hence, the number of distinct icosahedral clusters (N_{ICOC}) decreases in general (Fig. 4(a)). However, it can be seen that the increase in FI% does not necessary imply a larger (N_{ICOC} or a larger LCC. For example, 1% increase in FI% from $Cu_{46}Zr_{54}$ to $Cu_{50}Zr_{50}$ correspond to increase in (N_{ICOC} from 30 to 36. The LCC, however, show a small decrease in size from 25 to 22. In the case of $Cu_{46}Zr_{54}$ and $Cu_{50}Zr_{50}$ glasses with the FI population of 6.9% and 10.2%, respectively, the (N_{ICOC} differs by just one cluster. However, the LCC in the latter is significantly larger (131) than the former (81) glass composition. For the Cu% >54 in the binary system, a rapid decrease and increase in (N_{ICOC}) and LCC, respectively is observed due to increase in the degree of interconnection among the FIs. In order to provide a visualization of the FI connectivity and the formation of backbone MRO structures, snapshots of the simulation box with one of the LCCs in the studied metallic glass compositions are given in Fig 5. For the clarity in understanding the degree of FI interconnectivity, only the central Cu atoms of the interconnected FIs are shown. It is evident that a backbone network of interconnected FIs that percolates over the volume of the Cu-Zr metallic glass with Cu% >54. While such a network of FIs play an important role in the drastic slowdown of the dynamics in the supercooled liquid region [14, 29], and hence glass formation, FIs are not the sole structure feature that completely accounts for the atomic-level structure and glass-forming ability of the Cu-Zr systems. $< 0, 2, 8, 2 >$ –also known as defected icosahedon–is another major polyhedron type that plays an important role in structure and dynamics of the these systems [53]. However, the FIs and the defected icosahedra together constitutes 80-88% of atoms of the systems. Therefore, a fundamental organization of these two polyhedra types in 3D space and the description of MRO becomes a complicated task. As a result, we have focussed on the MRO description solely based on the FIs, and explore the extent to which it is correlated with the global structure of the studied metallic glasses.

3.2 Zr-Cu-Al and Zr-Cu-Ag metallic glasses

Based on the literature, the structural and electronic correlations in Zr-Cu-Al and Zr-Cu-Ag metallic glasses fulfilled the Nagel-Tauc condition [54], $K_p = 2K_F$, relating the average structure of the glasses at the MRO scale corresponding to the position of the first peak of S(q) and the radius of the Fermi surface in the nearly-free electron framework. we found a definite role of the electronic structure in stabilization of the structure at the MRO level. In an earlier reported work on $Zr_{50}Cu_{45}Al_5$ and $Zr_{50}Cu_{45}Ag_5$, Al and Ag with different chemical-ordering tendencies have been found to give rise to a qualitatively different MRO [55]. The Al-bearing system has been reported to show a dominant icosahedral ordering, while the other system with Ag demonstrates crystal-like MRO with a smaller degree of icosahedral order. However, the details of the difference in the 3D structure at the MRO scale in two metallic glass systems remain to be elucidated. As Al and Ag exhibit the hetero-coordination and homo-coordination tendencies, respectively, it would be really interesting to look into the difference in the organization of the dominant local structural features at the MRO scale in the two ternary metallic glass systems.

We begin with the examination of the population of the different Voronoi polyhedra types in the $Zr_{50}Cu_{40}Al_{10}$, $Zr_{50}Cu_{40}Ag_{10}$, $Cu_{50}Zr_{40}Al_{10}$, and $Cu_{50}Zr_{40}Ag_{10}$ metallic glasses shown in Fig. 7. It can be seen that the five-fold faces, in general, dominate the short-range order polyhedral structures. $< 0, 2, 8, 1 >$, $< 0, 2, 8, 2 >$ and $< 0, 0, 12, 0 >$ are the most dominant Voronoi polyhedra types in all the four metallic glasses. The population of $< 0, 0, 12, 0 >$–the so-called FI–significantly differs in the four metallic glasses, the highest in one $Cu_{50}Zr_{40}Al_{10}$ and the lowest in $Zr_{50}Cu_{40}Ag_{10}$. Therefore, we single out the FIs for further investigations and segregate the populations of Cu-centred, Zr-centred, Al-centred and Ag-centred FIs as shown in Fig. 8. It can be observed that major fraction of the FI population in all the four glasses is Cu-centred, and Cu-rich compositions have larger proportions of FIs than the Zr-rich compositions. The presence of a significant number of Al-centred FIs compared to a very small num-

International Journal of Engineering Research & Technology (IJERT)
ISSN: 2278-0181
Vol. 15 Issue 05 , May - 2026

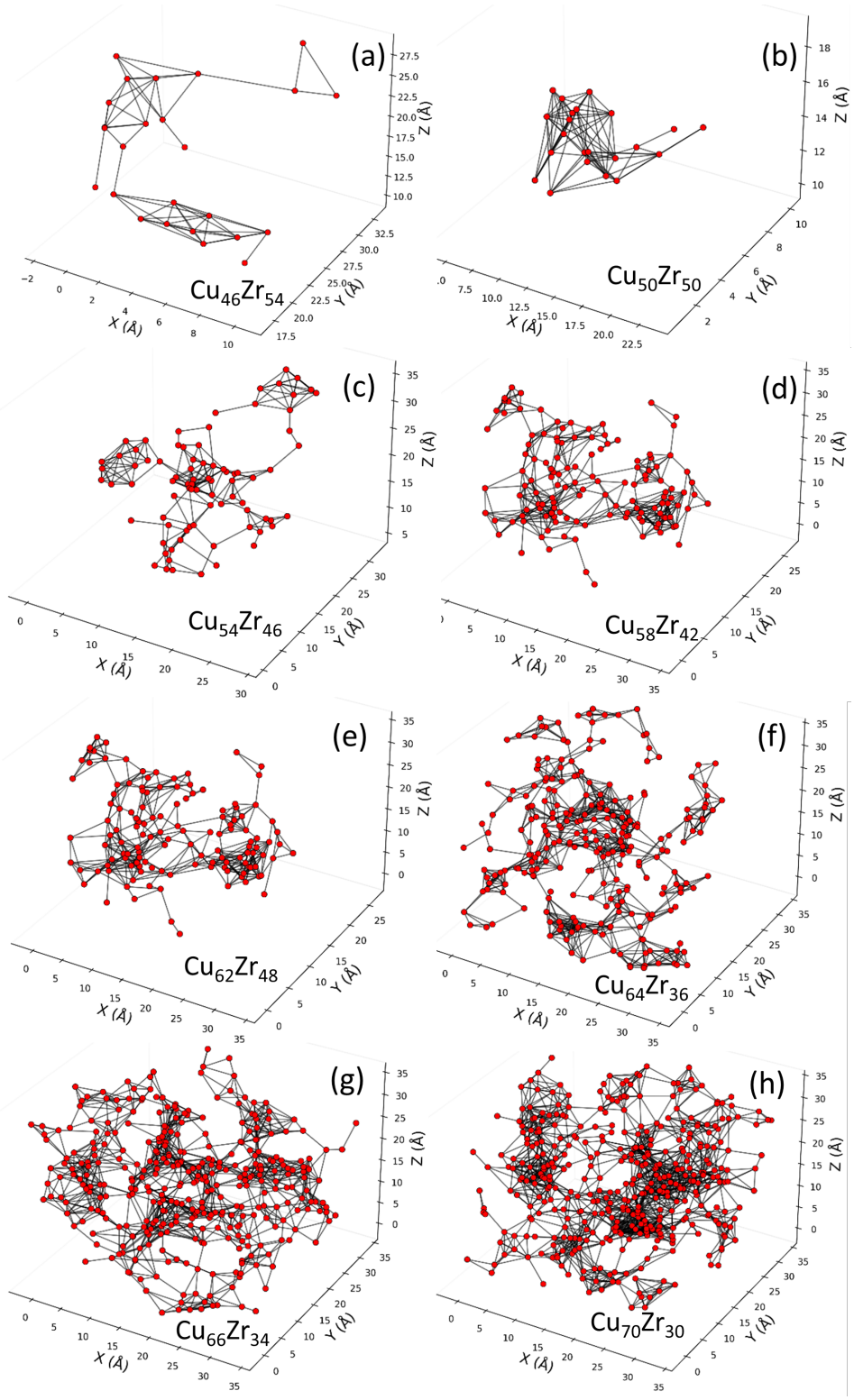

Figure 5: Snapshots of the simulation box with the central Cu atoms of a LCC in the studied Cu-Zr glass compositions. Only the central Cu atoms of the FIs are shown for clarity in understanding.

ber of Ag-centred FIs points to a key difference in the SRO and MRO in the Zr-Cu-Al and Zr-Cu-Ag systems due to the difference in the chemical ordering despite the similar atomic sizes of Al and Ag atoms. The significant difference in the FI populations in the four metallic glasses is a testimony to the competing Zr-Cu, Zr-Al, Zr-Ag, Cu-Al, and Cu-Ag interactions, as discussed in the previous chapter.

We now investigate the impact of the qualitatively differ-

International Journal of Engineering Research & Technology (IJERT)
ISSN: 2278-0181
Vol. 15 Issue 05 , May - 2026

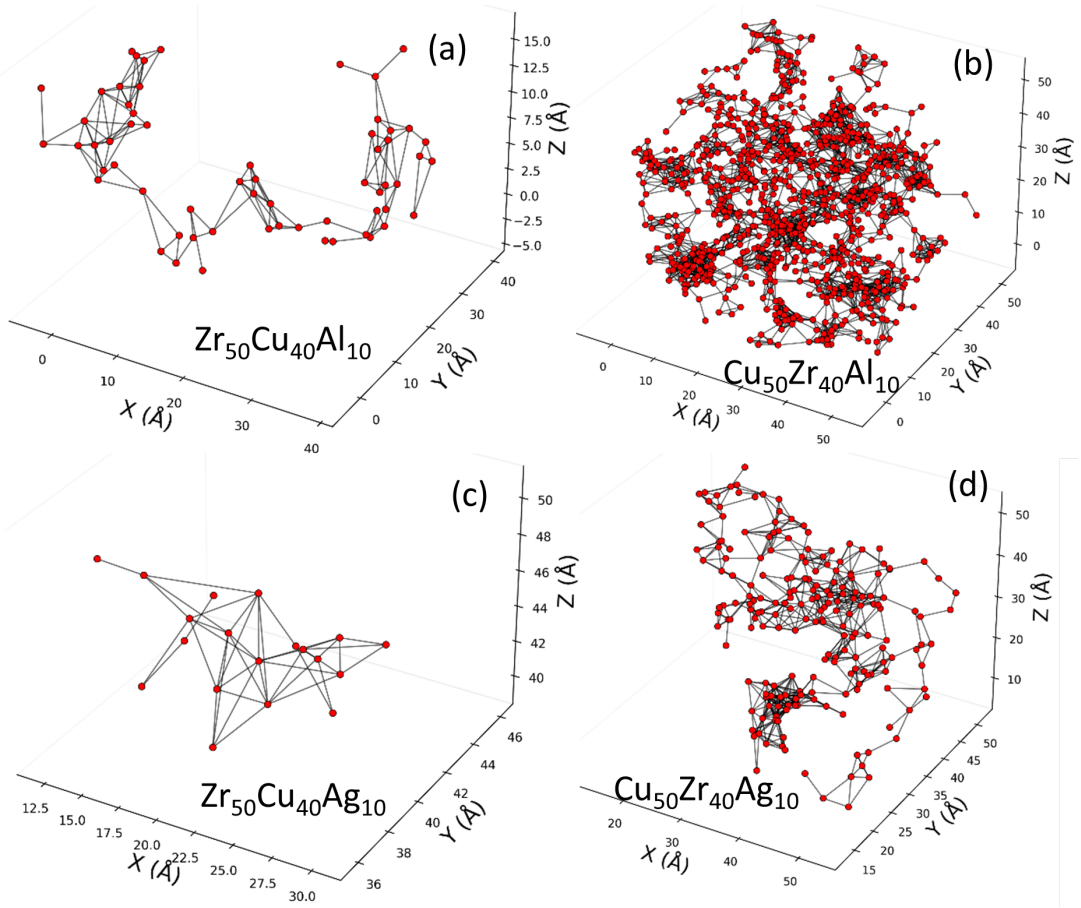

Figure 6: Snapshots of the simulation box with the central FI atoms of a LCC in, (a) $Zr_{50}Cu_{40}Al_{10}$, (b) $Zr_{50}Cu_{40}Ag_{10}$, (c) $Cu_{50}Zr_{40}Al_{10}$, and (d) $Cu_{50}Zr_{40}Ag_{10}$ Only the central atoms of the FIs are shown for clarity.

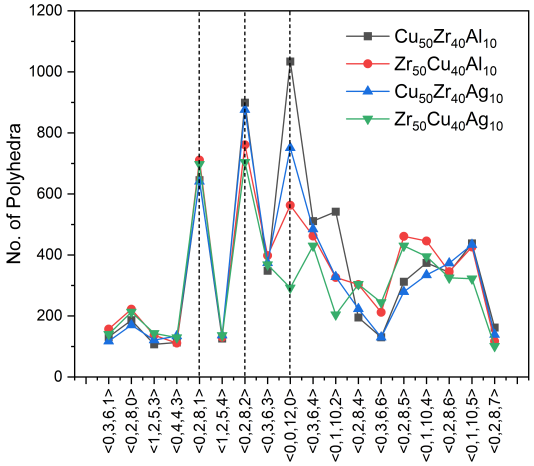

Figure 7: Population of the different Voronoi polyhedra types in $Zr_{50}Cu_{40}Al_{10}$, $Zr_{50}Cu_{40}Ag_{10}$, $Cu_{50}Zr_{40}Al_{10}$, and $Cu_{50}Zr_{40}Ag_{10}$ metallic glasses

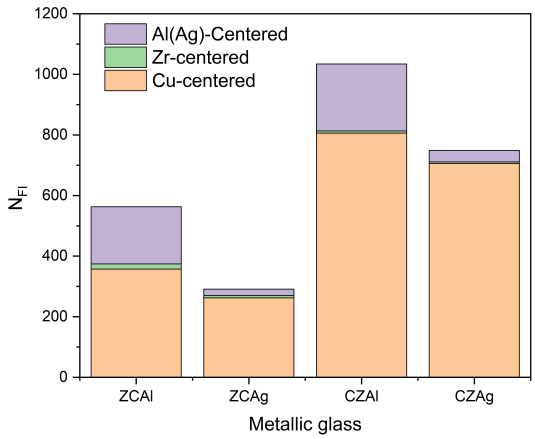

Figure 8: Populations of Cu-centred, Zr-centred, Al-centred and Ag-centred FIs in $Zr_{50}Cu_{40}Al_{10}$, $Zr_{50}Cu_{40}Ag_{10}$, $Cu_{50}Zr_{40}Al_{10}$, and $Cu_{50}Zr_{40}Ag_{10}$ metallic glasses

International Journal of Engineering Research & Technology (IJERT)
ISSN: 2278-0181
Vol. 15 Issue 05 , May - 2026

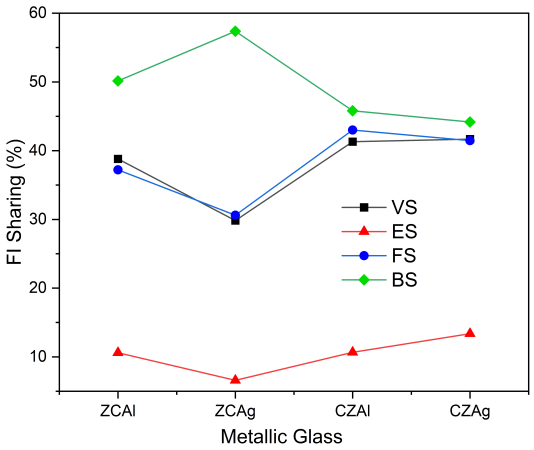

Figure 9: Percentage of FI connectivities through VS, ES, FS, and BS in $Zr_{50}Cu_{40}Al_{10}$ (ZCAl), $Zr_{50}Cu_{40}Ag_{10}$ (ZCAg), $Cu_{50}Zr_{40}Al_{10}$,(CZAl) and $Cu_{50}Zr_{40}Ag_{10}$ (CZAg) metallic glasses

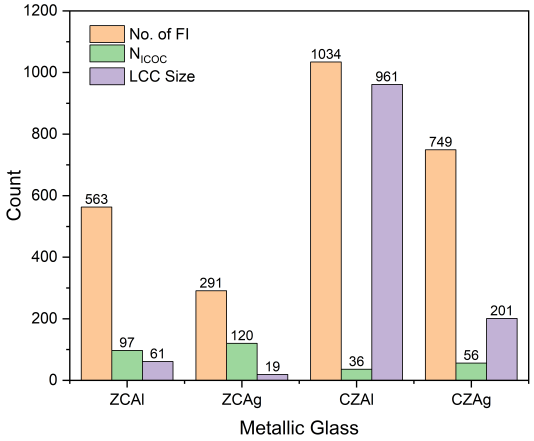

Figure 10: FI connectivity and MRO statistics in $Zr_{50}Cu_{40}Al_{10}$ (ZCAl), $Zr_{50}Cu_{40}Ag_{10}$ (ZCAg), $Cu_{50}Zr_{40}Al_{10}$,(CZAl) and $Cu_{50}Zr_{40}Ag_{10}$ (CZAg); FI population (N_{FI}) (orange), number of distinct FI clusters formed by FI sharing (N_{ICOC}) (green), and and the LCC size in terms of number of central FI atoms (purple).

ent chemical-ordering on the interconnectivity of the FIs in the Zr-Cu-Al and Zr-Cu-Ag systems. The percentage of FI connectivities through VS, ES, FS, and BS in $Zr_{50}Cu_{40}Al_{10}$ (ZCAl), $Zr_{50}Cu_{40}Ag_{10}$ (ZCAg), $Cu_{50}Zr_{40}Al_{10}$,(CZAl) and $Cu_{50}Zr_{40}Ag_{10}$ (CZAg) metallic glasses are shown in Fig. 9. As in the case of Cu-Zr metallic glasses(Fig.3), FI connectivity through BS and ES remain to be the most favoured and the least favoured connectivity mechanism, respectively. FS and VS connectivities are equally dominant. However, it should be noted that BS connectivity is preferred at the cost of the other three connectivity types in $Zr_{50}Cu_{40}Ag_{10}$. In this Zr-rich glass with the lowest population of FIs, it implies compact FI clustering, which could be attributed to the highly competing Zr-Cu and Zr-Ag interactions with their enthalpies of mixing of -23 kJ/mol and -20 kJ/mol, respectively. It also indicates the homo-coordination and phase separation tendencies of the Ag atoms. Such a compact FI clustering remains subdued in the Cu-rich $Cu_{50}Zr_{40}Ag_{10}$ glass due to larger concentration of Cu atoms and Cu-centred FIs. To gain further understanding of the organization of the FIs through the four connectivity mechanisms and the nature of MRO, we carry out an analysis of the number and size of the distinct clusters formed due to the interconnectivity of the FIs. The results are presented in Fig. 10. To complement these results and provide a better perspective of the organization of the FIs, LCC and MRO, snapshots of the simulation box with the central FI atoms of a LCC in the four metallic glasses are shown in Fig.6. It is evident that a relatively small number of distinct FI clusters, $N_{ICOC} = 36$, are formed in the Cu-rich $Cu_{50}Zr_{40}Al_{10}$ due to large FI connectivity among the highest number of FIs (1034). Largest connected clusters with the number of central atoms of FIs as large as 961 are formed as the icosahedral MRO pervades in this glass, as seen in Fig. 6(a). A larger number $N_{ICOC} = 56$ with a significantly small LCC size (201) in $Cu_{50}Zr_{40}Ag_{10}$ compared to $Cu_{50}Zr_{40}Al_{10}$ is a vindication of the compact FI clustering due to competing Zr-Cu and Zr-Ag interactions discussed earlier. Such a compact FI clustering in Ag-bearing ZrCu metallic glasses is further emphasized by the results for $Zr_{50}Cu_{40}Ag_{10}$ glass, where a large number of distinct FI clusters ($N_{ICOC} = 20$) with smaller LCC size of 19 are formed despite the smallest population of FI. The qualitative difference in the FI connectivity and the MRO in the ZCAl, ZCAg, CZAl and CZAg glasses can be gauged from the snapshots in Fig. 6. As FIs are the fundamental polyhedra types that are linked to the stabilization of the metallic liquids against crystallization in the supercooled region and their GFA, the present results of qualitatively distinct icosahedral MRO, owing to different chemical-ordering tendencies of a third element in the binary Zr-Cu system, are very useful in further exploration of the linkages of the different chemical ordering with the structure and dynamics. Nevertheless, mere exploration of FI connectivity and the icosahedral network do not provide a comprehensive understanding of the MRO in the present systems, as other polyhedra types with mixed four-fold, five-fold and six-fold geometrical symmetries $- < 0,2,8,1 >, < 0,2,8,2 >, < 0,2,8,4 >, < 0,2,8,5 >, < 0,2,8,6 >, < 0,3,6,3 >, < 0,3,6,4 >. < 0,1,10,2 >,$

International Journal of Engineering Research & Technology (IJERT)
ISSN: 2278-0181
Vol. 15 Issue 05 , May - 2026

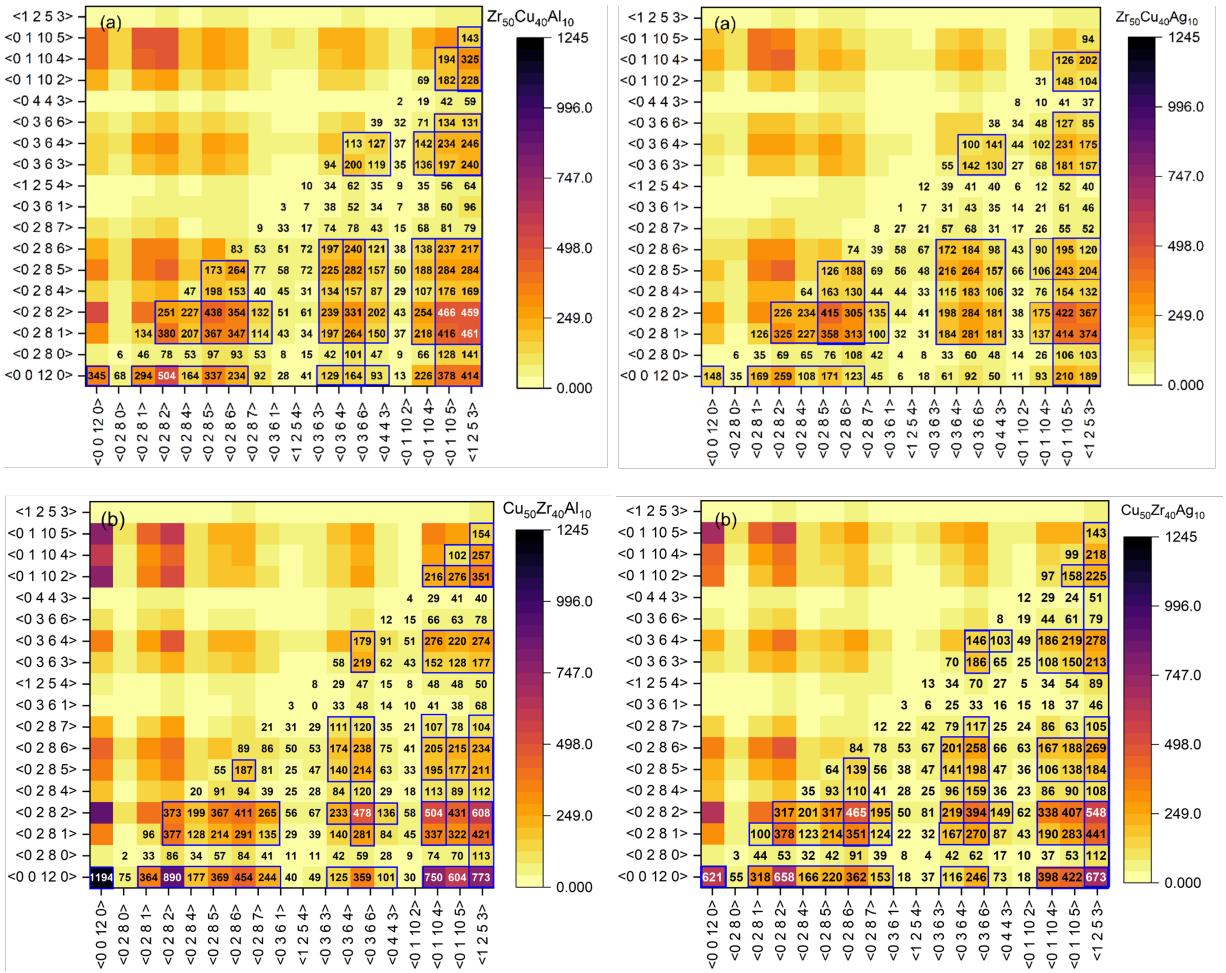

Figure 11: Statistical heat map of the interconnectivity of various polyhedra types in, (a) $Zr_{50}Cu_{40}Al_{10}$, and $Zr_{50}Cu_{40}Ag_{10}$ (b) $Cu_{50}Zr_{40}Al_{10}$ and $Cu_{50}Zr_{40}Ag_{10}$ glasses

$< 0, 1, 10, 4 >, < 0, 1, 10, 5 >$ – are also present in significant proportion, as shown in Fig. 7. A systemic organization of these polyhedra for the broader characterization of the MRO is a daunting task. However, investigation of the connectivity of each of these polyhedra (including FI) with the other polyhedra would provide a useful qualitative estimates of the relative degrees of the icosahedral MRO and crystal-like MRO in the studied metallic glass systems. To this end, we plot the statistical heat maps of the connectivity of the different polyhedra types. The results for the Zr-Cu-Al and the Zr-Cu-Ag systems are shown in Fig. 11, respectively. The color-coded blocks (with numbers) on the grid indicate the degree of connectivity among the pairs of given polyhedra types. The darker the block color, the higher the connectivity and vice-versa. The first feature in the heat maps that we would like to point out, is the FI $(0, 0, 12, 0–0, 0, 12, 0)$ connectivity in the four metallic glasses. The high FI connectivity in $Cu_{50}Zr_{40}Al_{10}$ and $Cu_{50}Zr_{40}Ag_{10}$ (Fig. 11(b)) as well as the low FI connectivity in $Zr_{50}Cu_{40}Al_{10}$ and $Zr_{50}Cu_{40}Ag_{10}$ (Fig. 11(a)) is the confirmation of the FI connectivity analysis presented in Fig. 10. It can be observed from the lowest row of the grid corresponding to the connectivities of $< 0, 0, 12, 0 >$ with the other polyhedra types in the Cu-rich glasses (CZAl and CZAg) that the FIs demonstrate high degrees of connectivities with $< 0, 2, 8, 1 >$, $< 0, 2, 8, 2 >$, $< 0, 2, 8, 4 >$, $< 0, 2, 8, 5 >$, $< 0, 2, 8, 6 >$, $< 0, 2, 8, 7 >$, $< 0, 3, 6, 4 >$, $< 0, 3, 6, 6 >$, $< 0, 1, 10, 4 >$, and $< 0, 1, 10, 5 >$. Apart from this, the high connectivities among the polyhedra types, separately marked by the blocks on the heat maps, indicate high degree of icosahedral ordering in CZAl and CZAg glasses. A bird's eye view of the heat maps suggests a larger diversity of the polyhedra connectivities i.e. a larger degree of disorder in these Cu-rich glasses. In the case of Zr-rich ZCAl and ZCAg glasses, where the icosahedral ordering is significantly lower, the larger connectivities among the polyhedra types with mixed four-fold, five-fold and six-fold geometrical symmetries indicate a significant crystal-like ordering. A higher degree of crystal-like ordering in ZCAg is clearly fathomable from the heat map (Fig. 11(a & b)) with the least diversity of the polyhedra connectivities compared to the other three glasses. Present findings of higher icosahedral MRO in CZAl glass compared to higher crystal-like MRO is in agreement with the similar findings reported based on the analysis of the global structure [55].

International Journal of Engineering Research & Technology (IJERT)
ISSN: 2278-0181
Vol. 15 Issue 05 , May - 2026

4. CONCLUSION

In this study, a detailed investigation of medium-range ordering (MRO) in binary Cu–Zr and ternary Zr–Cu–M (M = Al, Ag) metallic glasses has been carried out through a systematic analysis of the interconnectivity of full icosahedra (FI), ⟨0,0,12,0⟩ polyhedra, and their clustering behavior. The results establish that MRO in these systems is governed not merely by the presence of dominant short-range structural motifs but more importantly by their spatial organization, connectivity mechanisms, and the resulting network topology.

For the binary Cu–Zr metallic glasses, the analysis of FI connectivity reveals that bi-cap sharing (BS), face-sharing (FS), and vertex-sharing (VS) are the dominant interconnection mechanisms, while edge-sharing (ES) remains least favorable due to its incompatibility with efficient dense packing. The distributions of central atom pair distances corresponding to these connectivity types provide a direct structural interpretation of features observed in the pair distribution function (g(r)), particularly the sub-structure of the second peak. The persistence of peak positions across compositions indicates the existence of a robust geometrical backbone of interconnected icosahedra at the MRO scale .

A key outcome of the compositional study is the strong correlation between Cu content, FI population, and the extent of MRO. With increasing Cu concentration, there is a significant rise in FI population, leading to enhanced interconnectivity and the formation of larger icosahedral clusters. This is quantitatively reflected in the rapid growth of the largest connected cluster (LCC) and a concurrent reduction in the number of distinct clusters (N_{ICOC}). For Cu-rich compositions (Cu% >54), a percolating network of interconnected FIs emerges, forming a backbone structure extending over nanometer length scales. Such networks are closely associated with enhanced atomic packing efficiency, higher mass density, and improved glass-forming ability, particularly near compositions such as $Cu_{50}Zr_{50}$ and $Cu_{64}Zr_{36}$.

In the ternary Zr–Cu–Al and Zr–Cu–Ag systems, the role of chemical ordering becomes crucial in determining the nature of MRO. Despite similar atomic sizes of Al and Ag, their distinct chemical affinities lead to qualitatively different structural organizations. Al promotes hetero-coordination and enhances the formation and connectivity of Cu-centered icosahedra, resulting in a pronounced icosahedral MRO with large, percolating FI clusters, particularly in Cu-rich compositions such as $Cu_{50}Zr_{40}Al_{10}$. In contrast, Ag exhibits a tendency toward homo-coordination and partial phase separation, leading to comparatively lower FI populations and more compact, weakly connected clusters. This results in a reduced extent of icosahedral MRO and a greater propensity for crystal-like ordering, especially in Zr-rich compositions such as $Zr_{50}Cu_{40}Ag_{10}$.

The connectivity statistics and cluster analysis further confirm that strong FI interconnectivity leads to fewer but significantly larger clusters, whereas weaker connectivity results in a higher number of smaller, isolated clusters. Heat map analysis of polyhedral connectivity demonstrates that Cu-rich alloys exhibit higher diversity and stronger interconnections among various polyhedra, indicative of enhanced icosahedral ordering, while Zr-rich systems show comparatively ordered arrangements involving mixed polyhedra, reflecting crystal-like MRO.

Overall, this study demonstrates that MRO in metallic glasses is a consequence of a complex interplay between local topology, chemical ordering, and compositional effects. The formation of extended networks of interconnected icosahedra serves as a structural backbone that governs glass formation, stability, and dynamical slowdown in the supercooled regime. However, it is also evident that a complete description of MRO cannot be restricted solely to FI networks, as other polyhedral types with mixed symmetries contribute significantly to the overall structural organization.

These findings provide a coherent framework linking composition, chemical interactions, and topological organization at the MRO scale, and offer important insights into the design of metallic glasses with tailored structural and functional properties.

References

[1] D. B. Miracle, “A structural model for metallic glasses,” *Nature Materials*, vol. 3, no. 10, pp. 697–702, Oct. 2004.

[2] H. W. Sheng, W. K. Luo, F. M. Alamgir, J. M. Bai, and E. Ma, “Atomic packing and short-to-medium-range order in metallic glasses,” *Nature*, vol. 439, no. 7075, pp. 419–425, Jan. 2006.

[3] D. B. Miracle, T. Egami, K. M. Flores, and K. F. Kelton, “Structural aspects of metallic glasses,” *MRS Bulletin*, vol. 32, no. 8, pp. 629–634, Aug. 2007.

[4] Y. Q. Cheng, E. Ma, and H. W. Sheng, “Atomic level structure in multicomponent bulk metallic glass,” *Phys. Rev. Lett.*, vol. 102, p. 245501, Jun 2009.

[5] D. Ma, A. D. Stoica, and X.-L. Wang, “Power-law scaling and fractal nature of medium-range order in metallic glasses,” *Nature Materials*, vol. 8, no. 1, pp. 30–34, Jan. 2009. [Online]. Available: https://doi.org/10.1038/nmat2340

[6] X. J. Liu, Y. Xu, X. Hui, Z. P. Lu, F. Li, G. L. Chen, J. Lu, and C. T. Liu, “Metallic liquids and glasses: Atomic order and global packing,” *Phys. Rev. Lett.*, vol. 105, p. 155501, Oct 2010.

[7] A. Hirata, L. J. Kang, T. Fujita, B. Klumov, K. Matsue, M. Kotani, A. R. Yavari, and M. W. Chen, “Geometric frustration of icosahedron in metallic glasses,” *Science*, vol. 341, no. 6144, pp. 376–379, Jul. 2013.

[8] J. Ding and E. Ma, “Computational modeling sheds light on structural evolution in metallic glasses and supercooled liquids,” *npj Comput Mater*, vol. 3, no. 1, p. 9, Mar. 2017.

International Journal of Engineering Research & Technology (IJERT)
ISSN: 2278-0181
Vol. 15 Issue 05 , May - 2026

[9] Y. Yang, J. Zhou, F. Zhu, Y. Yuan, D. J. Chang, D. S. Kim, M. Pham, A. Rana, X. Tian, Y. Yao *et al.*, "Determining the three-dimensional atomic structure of an amorphous solid," *Nature*, vol. 592, no. 7852, pp. 60–64, 2021.

[10] Z. W. Wu, M. Z. Li, W. H. Wang, and K. X. Liu, "Correlation between structural relaxation and connectivity of icosahedral clusters in cuzr metallic glass-forming liquids," *Phys. Rev. B*, vol. 88, p. 054202, Aug 2013.

[11] Z. Wu, M. Li, W. Wang, and K. Liu, "Hidden topological order and its correlation with glass-forming ability in metallic glasses," *Nature communications*, vol. 6, no. 1, p. 6035, 2015.

[12] R. Soklaski, Z. Nussinov, Z. Markow, K. F. Kelton, and L. Yang, "Connectivity of icosahedral network and a dramatically growing static length scale in cu-zr binary metallic glasses," *Phys. Rev. B*, vol. 87, p. 184203, May 2013.

[13] J. Ding, Y.-Q. Cheng, and E. Ma, "Full icosahedra dominate local order in cu64zr34 metallic glass and supercooled liquid," *Acta Materialia*, vol. 69, pp. 343–354, May 2014.

[14] Y. C. Hu, F. X. Li, M. Z. Li, H. Y. Bai, and W. H. Wang, "Five-fold symmetry as indicator of dynamic arrest in metallic glass-forming liquids," *Nature Communications*, vol. 6, no. 1, p. 8310, Sep. 2015.

[15] Z. W. Wu, W. Kob, W.-H. Wang, and L. Xu, "Stretched and compressed exponentials in the relaxation dynamics of a metallic glass-forming melt," *Nature communications*, vol. 9, no. 1, p. 5334, 2018.

[16] Y. Cheng and E. Ma, "Atomic-level structure and structure–property relationship in metallic glasses," *Progress in materials science*, vol. 56, no. 4, pp. 379–473, 2011.

[17] P. F. Guan, T. Fujita, A. Hirata, Y. H. Liu, and M. W. Chen, "Structural origins of the excellent glass forming ability of $\mathrm{pd_{40}ni_{40}p_{20}}$," *Phys. Rev. Lett.*, vol. 108, p. 175501, Apr 2012.

[18] N. Mauro, M. Blodgett, M. Johnson, A. Vogt, and K. Kelton, "A structural signature of liquid fragility," *Nature communications*, vol. 5, no. 1, p. 4616, 2014.

[19] H.-K. Kim, J.-P. Ahn, B.-J. Lee, K.-W. Park, and J.-C. Lee, "Role of atomic-scale chemical heterogeneities in improving the plasticity of cu-zr-ag bulk amorphous alloys," *Acta Materialia*, vol. 157, pp. 209–217, 2018.

[20] Y.-C. Hu and H. Tanaka, "Physical origin of glass formation from multicomponent systems," *Science advances*, vol. 6, no. 50, p. eabd2928, 2020.

[21] K. Nomoto, A. V. Ceguerra, C. Gammer, B. Li, H. Bilal, A. Hohenwarter, B. Gludovatz, J. Eckert, S. P. Ringer, and J. J. Kruzic, "Medium-range order dictates local hardness in bulk metallic glasses," *Materials today*, vol. 44, pp. 48–57, 2021.

[22] E. Ma, "Tuning order in disorder," *Nature materials*, vol. 14, no. 6, pp. 547–552, 2015.

[23] T. Fujita, K. Konno, W. Zhang, V. Kumar, M. Matsuura, A. Inoue, T. Sakurai, and M. W. Chen, "Atomic-scale heterogeneity of a multicomponent bulk metallic glass with excellent glass forming ability," *Phys. Rev. Lett.*, vol. 103, p. 075502, Aug 2009.

[24] H. Fang, X. Hui, G. Chen, and Z. Liu, "Al-centered icosahedral ordering in cu46zr46al8 bulk metallic glass," *Applied Physics Letters*, vol. 94, no. 9, 2009.

[25] M. Wakeda and Y. Shibutani, "Icosahedral clustering with medium-range order and local elastic properties of amorphous metals," *Acta Materialia*, vol. 58, no. 11, pp. 3963–3969, 2010.

[26] Z. D. Sha, B. Xu, L. Shen, A. H. Zhang, Y. P. Feng, and Y. Li, "The basic polyhedral clusters, the optimum glass formers, and the composition-structure-property (glass-forming ability) correlation in Cu-Zr metallic glasses," *Journal of Applied Physics*, vol. 107, no. 6, p. 063508, 03 2010.

[27] X. Fang, C.-Z. Wang, S. Hao, M. J. Kramer, Y. Yao, M. I. Mendelev, Z. Ding, R. E. Napolitano, and K.-M. Ho, "Spatially resolved distribution function and the medium-range order in metallic liquid and glass," *Scientific reports*, vol. 1, no. 1, p. 194, 2011.

[28] Z. Sha, H. Pan, Q. Pei, and Y. Zhang, "The nature of the atomic-level structure in the cu-zr binary metallic glasses," *Intermetallics*, vol. 26, pp. 8–10, 2012.

[29] K. N. Lad, N. Jakse, and A. Pasturel, "Signatures of fragile-to-strong transition in a binary metallic glass-forming liquid," *The Journal of Chemical Physics*, vol. 136, no. 10, Mar. 2012.

[30] D. Wen, P. Peng, Y. Jiang, and R. Liu, "On the heredity and evolution of icosahedral clusters during the rapid solidification of liquid cu50zr50 alloys," *Journal of non-crystalline solids*, vol. 378, pp. 61–70, 2013.

[31] J. Zemp, M. Celino, B. Schönfeld, and J. F. Löffler, "Icosahedral superclusters in $\mathrm{cu_{64}zr_{36}}$ metallic glass," *Phys. Rev. B*, vol. 90, p. 144108, Oct 2014.

[32] P. Zhang, J. J. Maldonis, M. Besser, M. Kramer, and P. M. Voyles, "Medium-range structure and glass forming ability in zr–cu–al bulk metallic glasses," *Acta Materialia*, vol. 109, pp. 103–114, 2016.

International Journal of Engineering Research & Technology (IJERT)
ISSN: 2278-0181
Vol. 15 Issue 05 , May - 2026

[33] A. K. A. Lu, K. Nishio, T. Morishita, K. Ohara, Z. Lu, and A. Hirata, "Frank-kasper z16 local structures in cu-zr metallic glasses," *Phys. Rev. B*, vol. 102, p. 184201, Nov 2020.

[34] K. N. Lad and K. G. Soni, "Effect of al addition on structure and dynamics of zr-cu-al glass-forming alloy," *Materials Today: Proceedings*, vol. 47, pp. 546–550, 2021.

[35] Z.-Y. Zhou, Q. Yang, and H.-B. Yu, "Toward atomic-scale understanding of structure-dynamics-properties relations for metallic glasses," *Progress in Materials Science*, vol. 145, p. 101311, Oct. 2024.

[36] A. P. Thompson, H. M. Aktulga, R. Berger, D. S. Bolintineanu, W. M. Brown, P. S. Crozier, P. J. in't Veld, A. Kohlmeyer, S. G. Moore, T. D. Nguyen, R. Shan, M. J. Stevens, J. Tranchida, C. Trott, and S. J. Plimpton, "Lammps - a flexible simulation tool for particle-based materials modeling at the atomic, meso, and continuum scales," *Computer Physics Communications*, vol. 271, p. 108171, 2022.

[37] S. Nosé, "A unified formulation of the constant temperature molecular dynamics methods," *The Journal of Chemical Physics*, vol. 81, no. 1, pp. 511–519, 07 1984.

[38] W. G. Hoover, "Canonical dynamics: Equilibrium phase-space distributions," *Phys. Rev. A*, vol. 31, pp. 1695–1697, Mar 1985.

[39] L. Verlet, "Computer "experiments" on classical fluids. I. thermodynamical properties of Lennard-Jones molecules," *Physical Review*, vol. 159, no. 1, pp. 98–103, 1967.

[40] M. R. Hestenes and E. Stiefel, "Methods of conjugate gradients for solving linear systems," *Journal of Research of the National Bureau of Standards*, vol. 49, no. 6, pp. 409–436, 1952.

[41] D. J. Wales, *Energy Landscapes: Applications to Clusters, Biomolecules and Glasses*. Cambridge: Cambridge University Press, 2003.

[42] F. H. Stillinger and T. A. Weber, "Hidden structure in liquids," *Phys. Rev. A*, vol. 25, pp. 978–989, Feb 1982.

[43] C. H. Rycroft, "VORO++: A three-dimensional Voronoi cell library in C++," *Chaos: An Interdisciplinary Journal of Nonlinear Science*, vol. 19, no. 4, p. 041111, 10 2009. [Online]. Available: https://math.lbl.gov/voro++/

[44] F. C. Frank, "Supercooling of liquids," *Proceedings of the Royal Society of London A*, vol. 215, no. 1120, pp. 43–46, 1952.

[45] W. K. Luo, H. W. Sheng, F. M. Alamgir, J. M. Bai, J. H. He, and E. Ma, "Icosahedral short-range order in amorphous alloys," *Physical Review Letters*, vol. 92, no. 14, p. 145502, 2004.

[46] J. Ding, E. Ma, M. Asta, and R. O. Ritchie, "Second-nearest-neighbor correlations from connection of atomic packing motifs in metallic glasses and liquids," *Scientific reports*, vol. 5, no. 1, p. 17429, 2015.

[47] A. L. Greer, "Confusion by design," *Nature*, vol. 366, no. 6453, pp. 303–304, 1993.

[48] H. Shintani and H. Tanaka, "Frustration on the way to crystallization in glass," *Nature Physics*, vol. 2, no. 3, pp. 200–206, 2006.

[49] C. H. Bennett, "Serially deposited amorphous aggregates of hard spheres," *Journal of applied physics*, vol. 43, no. 6, pp. 2727–2734, 1972.

[50] K. Georgarakis, A. R. Yavari, D. V. Louzguine-Luzgin, J. Antonowicz, M. Stoica, Y. Li, M. Satta, A. LeMoulec, G. Vaughan, and A. Inoue, "Atomic structure of zr-cu glassy alloys and detection of deviations from ideal solution behavior with al addition by x-ray diffraction using synchrotron light in transmission," *Applied Physics Letters*, vol. 94, no. 19, p. 191912, 05 2009.

[51] Y. Li, Q. Guo, J. Kalb, and C. Thompson, "Matching glass-forming ability with the density of the amorphous phase," *science*, vol. 322, no. 5909, pp. 1816–1819, 2008.

[52] L. Yang, G. Q. Guo, L. Y. Chen, C. L. Huang, T. Ge, D. Chen, P. K. Liaw, K. Saksl, Y. Ren, Q. S. Zeng, B. LaQua, F. G. Chen, and J. Z. Jiang, "Atomic-scale mechanisms of the glass-forming ability in metallic glasses," *Phys. Rev. Lett.*, vol. 109, p. 105502, Sep 2012.

[53] K. Lad, "Correlation between atomic-level structure, packing efficiency and glass-forming ability in cu-zr metallic glasses," *Journal of Non-Crystalline Solids*, vol. 404, pp. 55–60, 2014.

[54] S. R. Nagel and J. Tauc, "Nearly-free-electron approach to the theory of metallic glass alloys," *Phys. Rev. Lett.*, vol. 35, pp. 380–383, Aug 1975.

[55] K. G. Soni, J. P. Anadani, and K. N. Lad, "Effect of chemical short-range ordering on thermodynamics, structure, and dynamics of zrcu-based metallic glass-forming liquids," *Journal of Applied Physics*, vol. 134, no. 23, 2023.